Pergamon

0042-6989(95)00264-2

Vision Res., Vol. 36, No. 14, pp. 2111–2120, 1996

Printed in Great Britain
0042-6989/96 $15.00 + 0.00

Limitations on Position Coding Imposed by Undersampling and Univariance

DENNIS M. LEVI*, STANLEY A. KLEIN†

Received 3 January 1994; in revised form 5 October 1995

Position judgments, which are exquisitely precise in the fovea, are markedly degraded in the periphery. In a recent article [Hess & Field (1993) *Vision Research, 33*, 2663–2670] argue that the poor representation of positional information in peripheral vision is a consequence of uncalibrated spatial disorder of cortical connections rather than due to undersampling of the retinal image. Specifically, Hess and Field argued that if positional uncertainty is due to undersampling, then because of univariance, there should be an associated contrast uncertainty. In this report we show that the univariance model is limited in its generality since: (1) the Hess and Field data in which contrast and position discrimination are decoupled do not preclude undersampling with large univariant filters; (2) aliasing can decouple position from contrast; (3) undersampling or noise at a second stage of processing can lead to selective losses of position information without any degradation of contrast information. Copyright © 1996 Elsevier Science Ltd.

Psychophysics Spatial sampling Position discrimination Contrast discrimination Spatial vision Univariance

INTRODUCTION

A longstanding interest of vision scientists is to relate the decline in visual function in peripheral vision to the eccentricity-dependent alterations which occur in anatomical structures and physiological functions (Weymouth, 1958; Rovamo *et al.*, 1978; Levi *et al.*, 1985; Drasdo, 1991). In the peripheral retina, there are marked variations in cone and ganglion cell size and spacing, and the arrangement of the sparsely sampled peripheral cones is much less regular than in the fovea. There are also marked alterations in size and sampling of cortical receptive fields in the periphery (e.g. Dow *et al.*, 1981).

Position judgments, which are exquisitely precise in the fovea, are markedly degraded in the periphery (e.g. Bourdon, 1902; Westheimer, 1982; Levi *et al.*, 1985; Hess & Watt, 1990; Hess & Field, 1993). Positional acuity falls off more rapidly with eccentricity than resolution or contrast detection (Westheimer, 1982; Levi *et al.*, 1985; Levi & Klein, 1992; Waugh & Levi, 1993; Levi & Waugh, 1994) and three main options have been proposed to account for this rapid fall-off of positional acuity:

1. Alterations in the size of retinal and cortical receptive fields (i.e. changes in the spatial scale of processing—Levi *et al.*, 1985; Levi & Waugh, 1994);
2. Alterations in the spacing of retinal and cortical receptors (i.e. undersampling—first suggested by Snyder, 1982; Levi & Klein, 1986; Lev *et al.*, 1987; Wilson, 1991); and
3. Topographical jitter in the positions of peripheral retinal cones or cortical receptive fields (i.e. uncalibrated jitter—Levi *et al.*, 1985; Hess & Watt, 1990; Wilson, 1991; Hess & Hayes, 1994).

In a recent article, Hess and Field (1993) argue that the poor representation of positional information in peripheral vision is a consequence of uncalibrated spatial disorder of cortical connections (the third option) rather than due to undersampling of the retinal image (the second option). Specifically, Hess and Field developed a model based on the well known principle of univariance. This principle, which has been central to our understanding of color vision, refers to the trade-off between stimulus properties such as wavelength and luminance, or position and stimulus contrast. Hess and Field argue that if positional uncertainty is due to undersampling, then there should be an associated contrast uncertainty. To test this idea, they measured position and contrast discrimination thresholds in the periphery with Gabor patches. Their results (discussed below) show that position discrimination is selectively degraded in the periphery, while contrast discrimination is not affected. Based on this result combined with their assumptions about the univariant nature of neurons, they conclude that spatial

*To whom all correspondence should be addressed at University of Houston, College of Optometry, Houston, TX 77204-6052, U.S.A.
†University of California, School of Optometry, Berkeley CA 94720-2020, U.S.A.

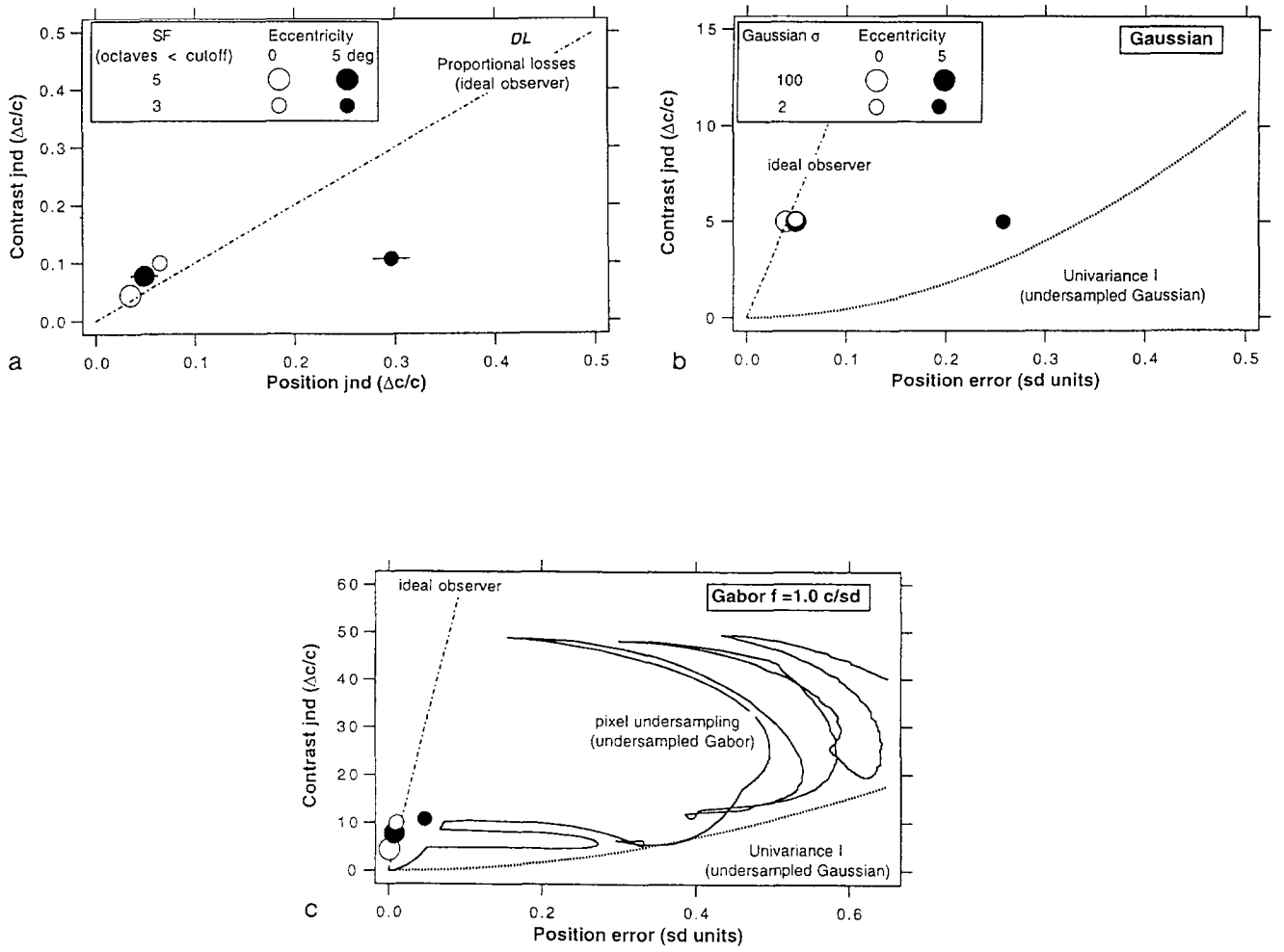

FIGURE 1. (a) Contrast discrimination threshold vs position discrimination threshold for abutting cosine gratings (contrast 80%) viewed either foveally (open symbols) or peripherally (eccentricity 5 deg in the lower visual field—solid symbols). The data are the Vernier thresholds of observer DL shown in Fig. 17 of Levi *et al.* (1994b). The peripheral contrast discrimination data (obtained under identical conditions) have not been shown previously. The spatial frequency was either 5 octaves (large symbols) or 3 octaves (small symbols) below the observer's resolution limit at each eccentricity. In the contrast jnd stimulus the sinusoidal test grating was added in-phase to the (sinusoidal) pedestal, whereas in the vernier stimulus the same test grating was added with an approximately 90 deg phase shift to the pedestal. Hu *et al.* (1993) were able to directly relate the vernier thresholds to contrast discrimination, by expressing both in the same units (Weber fractions, $\Delta C/C$). The thin dot-dashed curve illustrates proportional [equal in (a)] losses of position and contrast as predicted by an ideal observer model (Hu *et al.*, 1993). The foveal (open symbols) vernier and contrast jnds fall close to the thin dot-dashed line. At the lower spatial frequency (5 octaves below the cutoff, large symbols) the close similarity between position and contrast that is evident in foveal vision is also seen in peripheral vision (large solid circle in Fig. 1(a)]. At the higher spatial frequency (3 octaves below the cutoff shown by the small circles) the contrast jnd is similar in central and peripheral vision; however, in peripheral vision (and in strabismic amblyopes) the vernier Weber fraction for abutting sinusoidal gratings is markedly degraded. (b) Data of Hess and Watt (1990). The stimulus was a smooth undulation that was a Gaussian in the x direction with an offset that was a second derivative of a Gaussian in the y direction and they measured the threshold for discerning the offset as a function of Gaussian blur. This figure plots the thresholds (averaged across the two observers) obtained with a large amount of Gaussian blur (SD of 100 min) in the fovea (○) and periphery (4 deg eccentricity, ●). Hess and Watt did not measure contrast jnd, so we have assumed a value of 5% [similar to that measured by us at low spatial frequencies, and shown in Fig. 1(a)]. Their results show that there is very little loss of position acuity in the periphery for large amounts of blur. Interestingly, with small amounts of Gaussian blur (SD of 2 min), the peripheral thresholds at this eccentricity are about a factor of five worse than the foveal thresholds (○). The dot-dashed line illustrates proportional losses of position and contrast as predicted by an ideal observer model (Hu *et al.*, 1993) and shown in Fig. 1(a). The parabolic dotted line shows the prediction for Univariance I (mechanisms smaller than the stimulus envelope). Note that the Univariance I limit for position threshold is much larger than the very small loss of peripheral position acuity obtained with highly blurred stimuli. At low spatial frequencies neither undersampling nor position uncertainty are likely to degrade position discrimination, since performance will be limited by the stimulus blur (Snyder, 1982). (c) Replots the data of Fig. 1(a), assuming the stimulus to be a pair of abutting narrow band (1 c/SD) one-dimensional Gabor patches, since univariance modeling requires an envelope. We have assumed that the presence of the Gaussian envelope does not alter the thresholds for either the abutting Vernier or the contrast discrimination experiments. This assumption allows us to illustrate the relationship between contrast and position errors for the test-pedestal ideal observer model (thin dot-dashed straight line), and to compare them to the predictions of the Univariance I model based on undersampling a Gaussian (dotted line) or a Gabor [the solid curve in Fig. 1(c) labeled "pixel undersampling"]. This example shows that if the mechanisms are dense (left portion of curves) then both the position and the contrast of the Gabor function will be accurately judged. However, as the spacing between samples increases then the connection between the losses in position and contrast can become erratic.

undersampling is not the cause of increased position error with increasing eccentricity.

We believe that the issue is important, not only to understanding the factors that limit peripheral vision, but also amblyopic vision, since position discrimination is also much more degraded than contrast discrimination in amblyopes (Levi *et al.*, 1994b; Hess & Field, 1994). Therefore, the purpose of this report is to ask what constraints the principle of univariance imposes on position judgments. We shall argue that the principle of univariance has only limited applicability to understanding the limits of position acuity.

TWO DATA SETS

We begin by describing two sets of experiments which imply a decoupling of contrast and position information in peripheral vision; one set in which the features are closely spaced and the other set in which the features are widely separated. Several models for position discrimination, including the Hess and Field univariance model, will be described and finally we show the connection between the models and the experimental data.

Contrast discrimination and position discrimination with closely spaced features

For abutting, or closely spaced stimuli, there is an almost 1:1 relationship between position discrimination and contrast discrimination in the normal fovea. This close connection between position and contrast was demonstrated by Hu *et al.* (1993) who compared vernier acuity and contrast discrimination (jnd) in normal foveal viewing using abutting sinusoidal gratings. In the contrast jnd stimulus the sinusoidal test grating of contrast ΔC was added in-phase to the (sinusoidal) pedestal, whereas in the vernier stimulus the same test grating was added with approximately a 90 deg phase shift to the pedestal of contrast ΔC. Hu *et al.* were able to directly relate the vernier thresholds to contrast discrimination, by expressing both in the same units (Weber fractions ($\Delta C/C$). At low contrasts and for a mid range of spatial frequencies (5–10 c/deg) they found that vernier and contrast Weber fractions were approximately equal. The open circles in Fig. 1(a) illustrate foveal data for two spatial frequencies (5 and 3 octaves below the cutoff) obtained using the Hu *et al.* paradigm.* For this observer, both the vernier and contrast jnds fall close to the thin dot-dashed line of unity slope illustrating the equality between vernier jnd and contrast jnd predicted by Hu and colleagues' ideal observer model. In this figure, the large symbols are for a low spatial frequency grating (≈5 octaves below the observer's resolution limit). At low spatial frequencies, the close similarity between position and contrast that is evident in foveal vision is also seen in peripheral vision [5 deg in the lower visual field—solid large circle in Fig. 1(a)]. At low spatial frequencies neither undersampling nor position uncertainty are likely to degrade position discrimination, since performance will be limited by the stimulus blur (Snyder, 1982) rather than by disorder or undersampling of the receptor array.

A number of experiments show that for stimuli with little or no blur, position thresholds for abutting vernier targets are degraded in peripheral (or strabismic amblyopic) vision to a greater extent than resolution (Levi *et al.*, 1985) or Ricco's diameter (Levi *et al.*, 1994a). These studies, using abutting lines and edges all show about a 2–5-fold "extra" loss of position acuity (after accounting for reduced resolution and contrast sensitivity and increased spatial pooling) at an eccentricity of 5 deg. This extra loss is shown by the small circles in Fig. 1(a) which plot vernier and contrast jnds obtained using the Hu *et al.* (1993) paradigm at a spatial frequency 3 octaves below the observer's resolution limit in the fovea (small open circle) and periphery (5 deg lower field—small solid circle). Note that in peripheral vision [and in strabismic amblyopes (Levi *et al.*, 1994b)] the vernier Weber fraction for abutting sinusoidal gratings is markedly degraded, even after scaling for resolution, while the contrast Weber fraction is normal or nearly normal [see also Bradley & Ohzawa (1986); Legge & Kersten (1987)]. At 5 deg in the periphery, the "extra" loss of position acuity is about a factor of five when the spatial frequency of the stimulus is 3 octaves below the cutoff. This loss at middle spatial frequencies, and with localized stimuli (lines and edges), is of special interest to us because it is this type of loss that originally led us to suggest that spatial uncertainty and undersampling in peripheral vision might play a role in the extra loss of position acuity (Levi *et al.*, 1985).

Similar losses in peripheral position discrimination for closely spaced features were reported by Hess and Watt (1990). Rather than using a sharp vernier break as a target, Hess and Watt used a smooth undulation (a Gaussian in the x direction with an offset that was a second derivative of a Gaussian in the y direction) and measured the threshold for discerning the offset as a function of Gaussian blur at a large number of eccentricities. Their result, like the low spatial frequency data of Levi *et al.* (1994b) showed that for large amounts of blur (low spatial frequencies) there is no "extra" loss of position acuity. This result is illustrated in Fig. 1(b) for the fovea (large open circle) and the periphery [4 deg eccentric—large solid circle. Note that Hess and Watt did not measure contrast jnds, so we have plotted their data at contrast jnd values similar to those shown in Fig. 1(a)] and falls close to the dot-dashed line illustrating proportional losses of position and contrast. Interestingly, with small amounts of Gaussian blur, the peripheral thresholds at this eccentricity are about a factor of five worse than the foveal thresholds (small circles).

Contrast discrimination and position discrimination for well separated features

Hess and Field (1993) had observers make simulta-

*The data are the vernier thresholds of observer DL shown in Fig. 17 of Levi *et al.* (1994b) for high contrast (80%) cosine gratings. The peripheral contrast discrimination data (obtained under identical conditions) have not been shown previously.

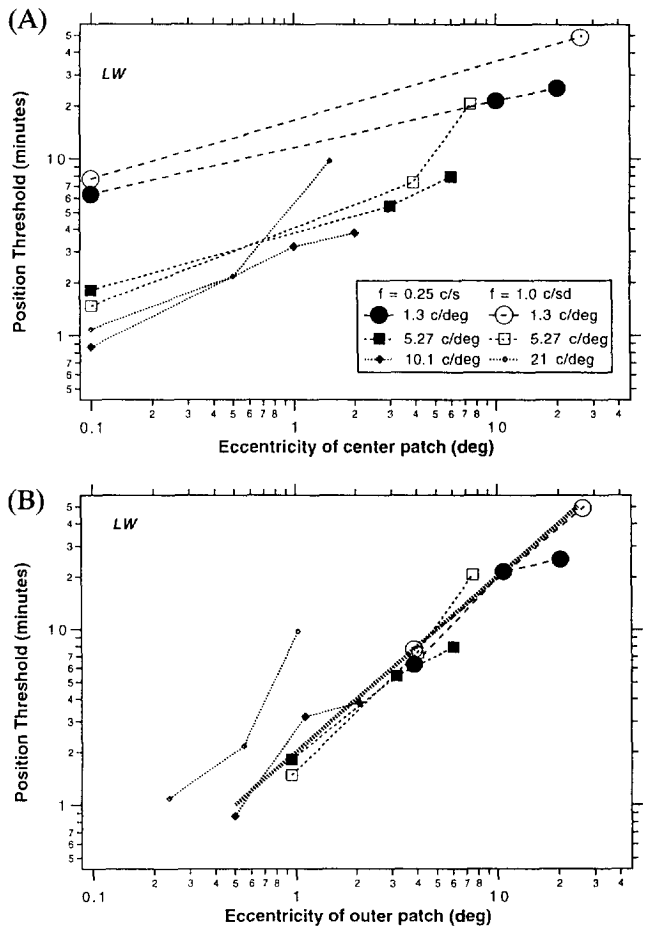

FIGURE 2. (A) All of the alignment data of one of Hess and Field's observers (LW) are summarized by plotting the alignment threshold against the eccentricity of the central patch. Open symbols are for a carrier frequency of $f = 1.0$ cycles per Gaussian standard deviation (1 c/SD); solid symbols are for $f = 0.25$ c/SD. Carrier spatial frequency is inversely proportional to symbol size. In this plot, it appears that thresholds depend on the spatial frequency and bandwidth (envelope size) of the stimuli. However, this picture is quite misleading (see text) because for a given eccentricity of the central patch the eccentricity of the outer patches varied over quite a large range due to the varying patch separations. (B) Replots the data of Fig. 2(A), using as the abscissa the eccentricity of the outer reference patches. Replotting the data in this way shows very clearly that the alignment thresholds increase in proportion to the eccentricity of the outer patches. With the exception of the 21 c/deg data (which were near the limit of visibility), thresholds are equal to about 1/30 of the eccentricity, quite independent of the carrier spatial frequency, bandwidth, envelope size, or separation. Thus, the main determinant of the position threshold is the eccentricity of the more peripheral features.

neous judgments of the relative position and the relative contrast of peripheral stimuli, and they compared the performance at different eccentricities. Their stimuli were three vertically separated Gabor patches, which varied in carrier spatial frequency, envelope size, and separation. The observers' task was to judge the alignment and contrast of the central patch compared to the outer patches (whose contrasts were fixed at 50 or 60%). The main result of Hess and Field's experiments is that position discrimination degrades with eccentricity, contrast discrimination does not. One of the most extreme examples of this decoupling of contrast and position is shown in Hess and Field's Fig. 5 for observer LW, where the position loss for a 5.27 c/deg carrier frequency at an eccentricity of 7.5 deg is more than a factor of 14 (open squares in our Fig. 2) greater than the foveal value, while the contrast jnd is unchanged.

Figure 2(A) replots all the alignment data of one of the Hess and Field observers (LW) by plotting the alignment threshold against the eccentricity of the *central* patch (Hess and Field specify eccentricity as the eccentricity of the central patch). In this plot, it appears that thresholds generally increase with eccentricity; however, it also appears that thresholds depend on the spatial frequency and bandwidth (envelope size) of the stimuli. In Fig. 2(B) the Hess and Field data are greatly simplified by replotting the data of Fig. 2(A), using as the abscissa the eccentricity of the *outer* reference patches (Klein & Levi, 1987; Levi & Klein, 1990). The *outer* patches limit position judgments since they are more eccentric, and therefore have greater position uncertainty than the less eccentric central patch. Replotting the data in this way shows very clearly that the alignment thresholds increase in proportion to the eccentricity of the outer patches. Although Hess and Hayes (1994) have argued that thresholds are dependent on stimulus size rather than eccentricity, recent experiments (Levi & Tripathy, 1995) show that when the standard deviation of the stimulus envelope (SD) is <1/5 the stimulus eccentricity (as was the case for most of the Hess and Field data), localization thresholds are independent of SD and are proportional to target eccentricity. It is only for larger values of SD that localization thresholds depend on the size of the stimulus envelope. With the exception of the 21 c/deg data (which is the one data set near the limit of visibility), thresholds are equal to about 1/30 of the eccentricity, quite independent of the carrier spatial frequency, bandwidth, or envelope size. Despite the large variation in position thresholds with eccentricity, this observer's contrast discrimination thresholds were, on average, about 11% independent of eccentricity.

Modeling the relationship between position and contrast: Undersampling and univariance

Two categories of univariance will be distinguished: Univariance I and II apply when the underlying mechanisms are smaller than, or larger than the stimulus respectively (we will discuss the case when the mechanism size is matched to the stimulus envelope later). It should be noted, however, that cortical neurons do not satisfy the principle of univariance, even if one considers only the spike rate (Albrecht & Geisler, 1994; W. Geisler, personal communication). Because of the contrast gain control, the trade-off between stimulus properties is much more constrained than that implied by univariance. For example, an optimal spatial frequency at medium contrast will produce a larger response than a nonoptimal spatial frequency at the highest possible contrast. The response to the nonoptimal stimulus saturates. This nonlinear behavior is a useful property in a population of cortical neurons for identifying stimuli independent of their contrast.

We will examine three reasons why univariance considerations have limited relevance for connecting position and contrast judgments.

1. In the Univariance I domain we show that undersampling with aliasing can produce a striking decoupling of position and contrast judgments.
2. In the Univariance II domain we show that different mechanism sizes can also decouple position from contrast. Undersampling with larger mechanisms, as found in the periphery, would produce greater uncertainty for position tasks (recall the lower panel of Fig. 2 which shows that the Hess and Field thresholds are proportional to the patch eccentricity).
3. Finally, there is evidence that position and contrast judgments are made at different stages of processing so that undersampling can affect each task differently.

Consider first Univariance I, where the mechanisms are much smaller than the stimulus. Hess and Field (1993) point out that if the judgment is based on the output of a single detector then there is a direct connection between position uncertainty and contrast. If the mechanism sampling is dense then the sample at the peak of the stimulus will measure the correct contrast and also will determine the correct location. However, if the sampling is sparse then the stimulus peak may be missed and errors will be found in both position and contrast. Since near the peak the stimulus has a parabolic shape, this univariance model is expected to produce a quadratic connection between position errors and contrast errors (with contrast errors being smaller).

Based upon their univariance model assumptions, Hess and Field argue that undersampling is not compatible with their data. We believe that there are several ways in which position discrimination can be selectively degraded, including undersampling. The intuition that undersampling should impair position judgments more than it impairs contrast judgments is based on our experience with undersampled gratings. In an aliased grating one can still make reasonably good contrast judgments, but the scrambled phases play havoc with position judgments. Consider, for example, the finding that detection thresholds fall very slowly with spatial frequency with interference fringes >60 c/deg (Williams, 1985) because the contrast signal is maintained by the undersampled array, whereas position information (grating orientation) is dramatically distorted (Williams, 1985, 1988).

In peripheral vision there is considerable evidence for undersampling and aliasing (Coletta & Williams, 1987; Coletta *et al.*, 1990). In order to illustrate the degree to which undersampling degrades contrast and position discrimination, we carried out a number of simulations using Gabor functions similar to those used by Hess & Field (1993). The Matlab code for all the simulations is given in Appendix A. The results of the simulations will be discussed below.

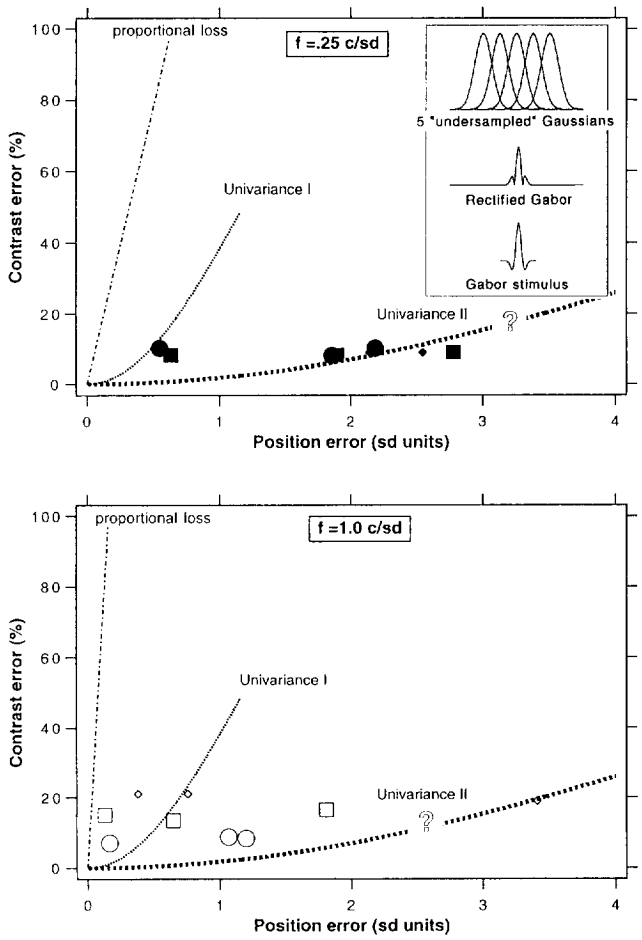

FIGURE 3. Position error vs contrast error according to three different model assumptions. The two panels correspond to carrier frequencies of 0.25 and 1.0 c/SD, corresponding to the broad bandwidth ($f = 0.25$ c/SD) and narrow bandwidth stimuli ($f = 1.0$ c/SD) used by Hess and Field. These figures plot contrast variability on the ordinate vs position variability on the abscissa with the sample spacing as the parameter that produces the range of values. Each panel shows three curves. The dot-dashed curve illustrates proportional losses of position and contrast. This curve is predicted by an ideal observer model (Hu *et al.*, 1993). The dotted line shows the prediction for Univariance I (mechanisms smaller than the stimulus envelope). The broad dotted curve represents the prediction of Univariance II, where the mechanisms are larger than the stimulus. We believe that Univariance II applies to the Hess and Field (1993) data. The horizontal position of the Univariance II curve is arbitrary, since it depends on the (unknown) size of the mechanisms selected for this task (thus the question mark). A model based on sampling with a filter matched to the stimulus (rather than the visual mechanism) will lie between the Univariance I and Univariance II curves. The symbols are the data of LW from Hess and Field (1993). The inset illustrates the relationship between stimulus size and mechanism size for Univariance II. The top row of the inset shows five Gaussian "mechanisms", with uniform spacing equal to 2 SD, i.e. "undersampled". The bottom row of the inset shows the broadband ($f = 0.25$ c/SD) Gabor stimulus of Hess and Field with a standard deviation equal to half that of the Gaussian mechanisms. The middle row shows a rectified Gabor stimulus. This rectification stage is necessary so that the Gaussian mechanisms can "see" the stimulus.

The structure of our simulations was similar to the model described by Hess & Field (1994). Specifically, we assumed a uniformly spaced array of receptive fields which vary in size and sampling density to simulate variations with eccentricity. For Univariance I, the receptive fields are assumed to be smaller than the

stimulus (points); for Univariance II, the receptive fields are assumed to be larger than the stimulus (Gaussians). The stimulus is presented at random locations with respect to the array of receptive fields. For our calculations we sampled the stimulus with a uniform sampling for each sample spacing. Five hundred different initial phases were chosen for the sampling array, uniformly spaced in order to obtain the full range of aliased patterns. The model that we use for estimating contrast and position thresholds is simple-minded, and the gory details and Matlab code are given in Appendix A. For each sampling phase we take the magnitude of the sample with maximum absolute value as an estimate of the contrast of the patch, and the location of that sample as an estimate of the patch position. The standard deviation of the 500 position estimates is taken to be the position error. The standard deviation of the contrast estimates divided by the mean of the contrast estimates is taken to be the contrast error. The parabolic lines in Figs 1 and 3 labeled Univariance I show the connection between position and contrast for a Gaussian (or Gabor) stimulus. The solid (erratic) line in Fig. 1(c) labeled "pixel undersampling" shows how contrast and position errors covary when a Gabor stimulus is undersampled (to be discussed below). The simulations are not meant to be a quantitative model of position and contrast discrimination. Rather, the goal was to show that undersampling can lead to a decoupling of contrast and position, contrary to the claims of Hess and Field, while still not violating univariance constraints.

CONNECTING THE MODELS TO THE EXPERIMENTS

Application to abutting, minimally blurred, local and sinusoidal stimuli

Figure 1(a) and (c) show vernier and contrast jnds for abutting sinusoids in foveal and peripheral vision. This task is in the Univariance I regime because the sinusoid is an extended stimulus, much larger than the mechanism receptive field. In the fovea (open circles) the vernier thresholds are very close to being equal to the contrast discrimination thresholds. As shown in Fig. 1(a), in peripheral vision (filled circles, and also in strabismic amblyopic vision) at medium spatial frequencies (e.g. 3 octaves below the cutoff) contrast discrimination thresholds are essentially normal, while the vernier thresholds are elevated by a factor of about five (the rightward filled circle).

Figure 1(c) replots the data of Fig. 1(a), but now the axes have been transformed into standard deviation units by assuming the stimulus to be a pair of abutting narrow band (1 cycle/standard deviation) one-dimensional Gabor patches. We have assumed that the presence of the Gaussian envelope (needed for converting the sinusoidal test pattern to a Gabor stimulus) does not alter the thresholds for either the abutting vernier or the contrast discrimination experiments. This assumption allows us to illustrate the relationship between contrast and position errors for the test-pedestal ideal observer model (see Appendix B for details), and to compare them to the predictions of the Univariance I model. As will be discussed later, plotting the data on a SD abscissa can be misleading. The univariance model requires an envelope because the envelope provides the outer boundary of the position uncertainty. Specifically, the thin dot-dashed straight line in Fig. 1(c) shows the equality between vernier thresholds and contrast discrimination thresholds in the normal fovea. The "extra" degradation of position thresholds in peripheral (and strabismic amblyopic) vision is shown by the small filled circle, reminding us that the position error is five times larger than that of the fovea.

In going from Fig. 1(a) to (c) the abscissa values are divided by 2π since $T = \Delta C/C$ is equal to the threshold phase shift in radians [Hu *et al.*, 1993; and see Eqn (6) of Appendix B] or $T/2\pi$ when expressed in cycles. For the $f = 1.0$ c/sd Gabor stimulus used in Fig. 1(c), the threshold is also given by $T/2\pi$ SD units. These are the units used in Fig. 1(c) in order to match the univariance plots of Hess and Field. As an example the small filled circle in Fig. 1(a) has a position threshold in contrast units of $\Delta C/C = 0.3$. In Fig. 1(c) the threshold is 0.05 SD units.

The dotted line in Fig. 1(c) (the bottom curve) shows the prediction for Univariance I based on undersampling a Gaussian. This was calculated using the Matlab program (see Appendix A with the carrier frequency set to zero (the stimulus is a Gaussian). Our example of the abutting Gabor stimulus does not violate Univariance I, i.e. the erratic solid line is never to the right of the bottom (dotted) curve. Univariance states that the error in position is governed by the envelope of the stimulus (see the lower panel of Hess and Field's Fig. 1). This is a very conservative limit, and one that is not violated by our undersampled abutting stimulus example. For a narrow bandwidth stimulus in which the envelope standard deviation is equal to the carrier wavelength [as illustrated in Fig. 1(c)] the Univariance I limit on position thresholds would be about 30 times larger than the measured thresholds. Thus, the univariance limit is much larger than the 4–5-fold loss that we require to explain the loss of peripheral position acuity using abutting vernier stimuli in the Levi *et al.* (1994b) experiment described above. We should point out that if the Gaussian envelope were broader, the data and the ideal observer line would move to the left. If the Gaussian envelope were narrower (a broader bandwidth stimulus) the data and ideal observer line would move to the right; however, in that case we would not expect the sinusoidal data to be the same as the broad bandwidth Gabor data, because as the grating is reduced to a single bar there is a loss of redundancy and vernier thresholds may degrade.

The results of the Univariance I model (Appendix A as applied to the abutting Gabor stimulus is shown by the solid curve in Fig. 1(c) labeled "pixel undersampling" (i.e. it is the Univariance I prediction based on undersampling the Gabor). Note that for Gabor stimuli, undersampling can cause extra deficits for the contrast

task compared to the prediction for the broad bandwidth Gaussian stimulus. The unusually shaped oscillations in Fig. 1(c) are straightforward. The upper left tips of the "waves" occur when there are 1/2, 1, 3/2, and 2 c/sample. At these points the contrast fluctuations increase dramatically since the peak contrast goes all the way down to zero, and the position fluctuations decrease since "moiré" beats which can place the maximum in a distant cycle of the Gabor are avoided. This example shows that if the mechanisms are dense then both the position and the contrast of the Gabor function will be accurately judged. However, as the spacing between samples increases then the connection between the losses in position and contrast can become erratic. We want to strongly emphasize that we do not take this univariance model too seriously. Judging position and contrast based on the one sample with the greatest contrast is far from what an ideal observer would do. Also our assumption of uniformly spaced samples is not realistic. In further simulations with noise added to the position of the samples, we find the nonsmooth fluctuations are attenuated. This model is just presented to illustrate the degradations that can *in principle* be caused by undersampling, since Hess and Field gave an "in principle" argument that univariance produces a smooth coupling between contrast uncertainty and position uncertainty.

Application to well separated features: Univariance II

When the mechanism is much larger than the stimulus (Univariance II) one arrives at a very similar conclusion to the Univariance I case, except the roles of mechanism and stimulus are reversed. If the mechanisms are dense, then it is likely that the stimulus will fall near the peak of one of the mechanisms. However, if the mechanisms are sparse then the stimulus might fall away from a mechanism peak. Based on the univariance assumption (threshold based just on the output of a single optimal mechanism) there will be errors both in contrast and position. Clearly, this model is far from ideal; however, this is essentially the model proposed by Hess and Field (1993). We believe that Univariance II applies to the Hess and Field (1993) experiment (where the stimulus elements are well separated). We come to this conclusion because as is seen in our Fig. 2 the Hess and Field data only depend on the eccentricity of the stimulus (lower panel) and not on the size of the stimulus envelope. If the mechanisms had been smaller than or the same size as the stimulus then we would have expected there to be some dependence either on the spatial frequency or the envelope of the stimulus. A very simple explanation of the Hess and Field data is that in the periphery the mechanisms have a larger size, resulting in poorer position capabilities with no loss in contrast Weber fraction processing (Levi & Waugh, 1994, discussed further below).

Figure 3 shows the Hess and Field data (of LW), replotted in terms of the contrast error (%) vs the position error (in SD units) for both their broad bandwidth (A) and narrow bandwidth (B) stimuli, along with several model predictions. Univariance II leads to the predictions shown by the *broad dotted* curve in Fig. 3. Points along the curve are generated by different degrees of undersampling [the variable "samp(i)" of the Matlab program in Appendix A]. As the spacing between samples increases, losses can occur in judged position with much smaller losses in the accuracy of judging contrast. This example shows that undersampling can produce greater losses in position thresholds than are found in contrast thresholds (compare the Univariance curves to the proportional loss line). The position of the Univariance II curve in Fig. 3 was generated by scaling the Univariance I abscissa (the position error) by a constant factor (5 in Fig. 3). The scaling factor is arbitrary because we do not know the size of the mechanisms selected for this task in peripheral vision. With broadband stimuli, there is evidence from masking studies that larger (lower spatial frequency) mechanisms are selected for position judgments in peripheral (Levi & Waugh, 1994) and amblyopic (Levi, Waugh & Beard, 1994) vision. The larger the peripheral mechanism, the further to the right will be the Univariance II curve, and the more decoupled will be the position and contrast errors. A model based on sampling with a filter matched to the stimulus (rather than the eccentricity dependent visual mechanism) will lie between the Univariance I and Univariance II curves. However, in peripheral vision it is not clear that the filter selected matches the stimulus envelope, particularly when the stimulus is small (e.g. Hess and Field's broad bandwidth stimuli). Note that most of the Hess and Field data do not violate the Univariance II assumption [only one datum of LW and two data of RFH (not shown) fall below the line]. The constancy of the contrast discrimination data could be attributed to Weber noise that limits contrast discrimination (in both central and peripheral vision and in both eyes of amblyopes). The very degraded position thresholds are largely a consequence of the large mechanism size. Take as an example the rightmost datum in Fig. 3 (top), i.e. displaying the largest position error. This corresponds to data obtained with a broadband patch (5.27 c/deg) at a (center patch) eccentricity of 6 deg. The patch standard deviation was 2.85 min arc, thus the patch size was only about 1/125 of the target eccentricity, much smaller than the 1/5 of eccentricity where the stimulus size becomes significant in determining thresholds (Levi & Tripathy, 1995). The patch size is also very much smaller than the size of receptive fields which have been reported at this eccentricity (Dow *et al.*, 1981). Thus, we believe that these large position errors are an artifact of scaling by stimulus standard deviation. The actual threshold was in fact about 8 min arc or 1/45 of the target eccentricity. As shown in Fig. 2, under the conditions of Hess and Field's experiments, it is the target eccentricity, not the standard deviation which is important.

The key question raised by Hess and Field is whether the data violate the principle of univariance plus undersampling. Figure 3 suggests that the limitations imposed

by univariance depend rather critically upon assumptions about the size of the underlying mechanisms. The data of Hess and Field clearly violate Univariance I; however, without knowledge of the *mechanism* size (as opposed to the stimulus size), it is not possible to tell whether they violate Univariance II. Based upon our masking results, the most sensitive mechanisms for alignment at 5 deg in the periphery have a spatial period of about 15 min arc (Levi & Waugh, 1994), considerably larger than most of the envelope sizes chosen by Hess and Field. All of the broadband stimuli are smaller than 15 min arc, and only the narrowband (f = 1 c/SD), 1.3 c/deg data [open circles in Fig. 2(a)] had standard deviations larger than that. These are the data with the smallest thresholds (in SD units) and with the largest eccentricities (from 10 to 30 deg). The mechanisms at 10 and 30 deg are expected to be about two and six times larger than the mechanisms at 5 deg, respectively. The fact that the largest errors occur for broadband stimuli is consistent with the notion that the filter size is larger than the small Gaussian envelope selected by the experimenters. Given these uncertainties, univariance considerations do not seem to provide a very useful limit to position acuity.

The inset in Fig. 3 illustrates the relationship between stimulus size and mechanism size for Univariance II. Specifically, the top row of the inset shows five Gaussian "mechanisms", with uniform spacing equal to 2 SD, i.e. "undersampled". The bottom row of the inset shows the broadband (f = 0.25 c/SD) Gabor stimulus of Hess and Field. We have chosen a standard deviation equal to half that of the Gaussian mechanisms. The middle row shows a rectified (by plotting the absolute value) Gabor stimulus. This rectification stage is implicit in the local sign regime (i.e. where the stimulus features are well separated as in the Hess and Field experiment) and is necessary so that the low frequency mechanisms in the periphery can "see" the high frequency stimulus.* Rectification could be accomplished by the visual system in several ways [squaring, taking the absolute value, or Pythagorean summation of odd and even symmetric mechanisms (Klein & Levi, 1985)].

A two-stage model of position coding

Is undersampling necessary and/or sufficient for explaining the peripheral data? It is clearly not necessary since one can always come up with alternative methods such as spatial disorder for degrading position acuity. However, our modeling suggests that undersampling is sufficient for producing a greater loss in position acuity than what is expected from the contrast discrimination thresholds. There is an even stronger argument for how undersampling can lead to degraded position judgments without affecting contrast judgments. Even if Hess and Field had been correct that undersampling produces a tight connection between contrast and position discrimination, their data do *not* preclude undersampling. One plausible alternative explanation is that position processing is done at a second (or parallel) stage while contrast judgments are based on information from only the first stage. Thus, either undersampling, or noise at the second stage would have a differential effect upon position judgments. This second stage loss will degrade hyperacuity thresholds without affecting either contrast detection or contrast discrimination; since contrast discrimination was already accomplished at the first stage, position information would be selectively degraded. There are several lines of evidence which are compatible with a "second" stage computation. For example, Klein *et al.* (1974) argued that a second stage was needed for size judgments based on their observation of a decoupling between grating detection and the spatial frequency shift following adaptation. Indeed, Hess and Holliday (1992) have suggested a two-stage model for position judgments under conditions similar to those of Hess and Field (1993).

SUMMARY AND CONCLUSIONS

Hess and Field (1993) argue that the poor representation of positional information in peripheral vision is a consequence of uncalibrated spatial disorder of cortical connections rather than due to undersampling of the retinal image. Specifically, they argue that undersampling should have a predictable effect on contrast and position judgments. The main point of this article is not to argue in favor of undersampling†, but to argue that univariance considerations do not seem to provide a very useful limit to spatial vision and do not preclude undersampling as contributing to an extra degradation of position thresholds. Indeed, we have argued elsewhere that both undersampling *and* disorder may play a role in the extra loss of position acuity in periphery and strabismic amblyopia. In the present paper we showed how a model incorporating undersampling and large univariant mechanisms is sufficient to account for the decoupling of contrast and position reported by Hess and Field. As we pointed out above, plotting position thresholds in standard deviation units (as in Fig. 3) is quite misleading; the univariance predictions require assumptions about the mechanism standard deviation. As shown in Fig. 2, position thresholds (under the Hess and Field conditions) are determined by the stimulus eccentricity rather than by the stimulus standard deviation. In the "local sign" regime relevant to the Hess and Field stimuli, the rectified stimuli are processed by low spatial frequency mechanisms that are larger than the stimuli (Levi & Tripathy, 1995). Finally, we point out that position might be judged at a second (or independent) stage of processing, whereas contrast might be

*In their response to this paper, Field and Hess assert that our model involves a multilobed receptive field; however, that is clearly not the case, since the low spatial frequency filter will be able to 'see' the high spatial frequency target after the target is rectified.

†Having committed the sin of both undersampling, and topographical jitter as potential models for amblyopia, we are agnostic on this point.

judged at a first stage (Klein *et al.*, 1974). Undersampling at the second stage that degrades both position and contrast would only affect the position judgment since the contrast information was being used from the first stage. Thus, we conclude that the Hess and Field data do *not* preclude undersampling.

REFERENCES

Albrecht, D. G. & Geisler, W. S. (1994). Visual cortex neurons in monkey and cat: Contrast response nonlinearities and stimulus selectivity. *SPIE Proceedings* (Ed. Lawton T. B.), *2054*, 12–31.

Bourdon, B. (1902). La Perception Visuelle de l'Espace. Scheicher-Paris.

Bradley, A. & Ohzawa, I. (1986). A comparison of contrast detection and discrimination. *Vision Research*, *26*, 991–997.

Coletta, N. J. & Williams, D. R. (1987). Psychophysical estimate of extrafoveal cone spacing. *Journal of the Optical Society of America A*, *4*, 1503–1513.

Coletta, N. J., Williams, D. R. & Tiana, C. L. M. (1990). Consequences of spatial sampling for human motion perception. *Vision Research*, *30*, 1631–1648.

Dow, B. M., Snyder, R. G., Vautin, R. G. & Bauer, R. (1981). Magnification factor and receptive field size in foveal striate cortex of the monkey. *Experimental Brain Research*, *44*, 213–228.

Drasdo, N. & Cronly-Dillon, J. R. (1991). *The limits of vision*, 250–264. London: Macmillan.

Hess, R. F. & Field, D. (1993). Is the increased spatial uncertainty in the normal periphery due to spatial undersampling or uncalibrated disarray? *Vision Research*, *33*, 2663–2670.

Hess, R. F. & Field, D. (1994). Is the spatial deficit in strabismic amblyopia due to loss of cells or an uncalibrated disarray of cells? *Vision Research*, *34*, 3397–3406.

Hess, R. F. & Hayes, A. (1994). The coding of spatial position by the human visual system: Effects of spatial scale and retinal eccentricity. *Vision Research*, *34*, 625–643.

Hess, R. F. & Holliday, I. E. (1992). The coding of spatial position by the human visual system: Spatial scale and contrast. *Vision Research*, *32*, 1085–1097.

Hess, R. F. & Watt, R. J. (1990). Regional distribution of the mechanisms that underlie spatial localization. *Vision Research*, *30*, 1021–1031.

Hu, Q., Klein, S. A. & Carney, T. (1993). Can sinusoidal vernier acuity be predicted by contrast discrimination? *Vision Research*, *33*, 1241–1258.

Klein, S. A. & Levi, D. M. (1985). Hyperacuity thresholds of 1 second: theoretical predictions and empirical validation. *Journal of the Optical Society of America A*, *2*, 1170–1190.

Klein, S. A. & Levi, D. M. (1987). The position sense of the peripheral retina. *Journal of Optical Society of America A*, *4*, 1544–1553.

Klein, S. A., Stromeyer, C. F. & Ganz, L. (1974). The simultaneous spatial frequency shift: A dissociation between the detection and perception of gratings. *Vision Research*, *14*, 1421–1432.

Legge, G. E. & Kersten, D. (1987). Contrast discrimination in peripheral vision. *Journal of the Optical Society of America A*, *4*, 1594–1598.

Levi, D. M. & Klein, S. A. (1986). Sampling in spatial vision. *Nature*, *320*, 360–362.

Levi, D. M. & Klein, S. A. (1990). The role of separation and eccentricity in encoding position. *Vision Research*, *30*, 557–585.

Levi, D. M. & Klein, S. A. (1992). Local contrast and amblyopia. *Neuroscience Letters*, *136*, 63–66.

Levi, D. M., Klein, S. A. & Aitsebaomo, A. P. (1985). Vernier acuity, crowding and cortical magnification. *Vision Research*, *25*, 963–977.

Levi, D. M., Klein, S. A. & Wang, H. (1994a). Amblyopic and peripheral Vernier acuity: A test-pedestal approach. *Vision Research*, *34*, 3265–3292.

Levi, D. M., Klein, S. A. & Wang, H. (1994b). Discrimination of position and contrast in amblyopic and peripheral vision. *Vision Research*, *34*, 3293–3314.

Levi, D. M., Klein, S. A. & Yap, Y. L. (1987). Positional uncertainty in peripheral and amblyopic vision. *Vision Research*, *27*, 581–597.

Levi, D. M. & Tripathy, S. P. (1995). Spatial localization of a peripheral target: The role of spatial structure. *Investigative Ophthalmology Visual Science*, *36(Suppl)*, S835.

Levi, D. M. & Waugh, S. J. (1994). Spatial scale shifts in peripheral vernier acuity. *Vision Research*, *34*, 2215–2238.

Levi, D. M., Waugh, S. J. & Beard, B. L. (1994). Spatial scale shifts in amblyopic vision. *Vision Research*, *34*, 3315–3333.

Rovamo, J., Virsu, V. & Nasanen, R. (1978). Cortical magnification factor predicts the photopic contrast sensitivity of peripheral vision. *Nature*, *271*, 54–56.

Snyder, A. W. (1982). Hyperacuity and interpolation by the visual pathways. *Vision Research*, *22*, 1219–1220.

Waugh, S. J. & Levi, D. M. (1993). Visibility, luminance and vernier acuity. *Vision Research*, *33*, 527–538.

Westheimer, G. (1982). The spatial grain of the perifoveal visual field. *Vision Research*, *22*, 157–162.

Weymouth, F. W. (1958). Visual sensory units and the minimal angle of resolution. *American Journal of Ophthalmology*, *46*, 102–113.

Williams, D. R. (1985). Aliasing in human foveal vision. *Vision Research*, *25*, 195–205.

Williams, D. R. (1988). Topography of the foveal cone mosaic in the living human eye. *Vision Research*, *28*, 433–454.

Wilson, H. R. (1991). Model of peripheral and amblyopic hyperacuity. *Vision Research*, *31*, 967–982.

Acknowledgements—We are most grateful to David Field and Bill Geisler for several very helpful conversations aimed at clarifying the issues discussed here. We also thank Sarah Waugh, Srimant Tripathy, Alex Mussap, and Thom Carney for detailed comments and criticisms of an earlier version of this paper.

APPENDIX A

Matlab code for undersampling a Gabor function and generating Figs 1 and 3

```
1   nsamp=1000; nsamp2=500; freqs=[0 1];
2   for fi=1:2; freq=freqs(fi);
3     for i=1:nsamp; samp(i)=4*i/nsamp;
4       clear gabor;
5       for ph=1:nsamp2;
6         xs=(-3:samp(i):3). +ph*samp(i)/nsamp2;
7         gabor(ph,:)=exp(-xs.*xs/2).*cos(2*3.14159*freq*xs);
8         [mx(ph),pos(ph)]=max(abs(gabor(ph,:)));
9         pos(ph)=samp(i)*(pos(ph)+ph/nsamp2);
10      end
11      stdat(i,2*fi-1:2*fi)=std([100*mx', pos']);
12      stdat(i,2*fi-1)= stdat(i,2*fi-1)./mean(mx');
13    end
14  end
15  plot(stdat(:, 2),stdat(:, 1),stdat(:, 4),stdat(:, 3));
16  plot([0 1/(2*pi)],[0 100],'-.')
```

Explanation of each line of the above program.

1. The number of sample spacings and phase shifts are defined. Two carrier frequencies are calculated: $f = 0$ for the pure Gaussian Univariance I limit and 1.0 c/SD corresponding to the narrow bandwidth stimulus used by Hess & Field (1993). where SD is the standard deviation of the Gaussian envelope.
2. Iterate over the two carrier frequencies.
3. Iterate over the 1000 sample spacing that go from 0.004 to 4 SD units.

4. Clear the Gabor matrix since it changes size as the sample size changes.
5. Iterate over the 500 initial phases covering the full sample spacing.
6. The sample positions are defined. Samples go from −3 to +3 SD units.
7. The Gabor function is defined. The envelope has unity standard deviation.
8. The maximum value (mx) and index of the position (i_pos) of the maximum is calculated. The absolute value of the Gabor function is used since a wise observer would invert the sign of a negative sample.
9. The position of the maximum is converted from an integer to SD units.
11. The standard deviation of the maximum value (contrast) and position is calculated. The apostrophe means the transpose is needed because the standard deviation function (std) operates on columns but the original data had been in rows.
12. The contrast is normalized by the mean of the samples so that the contrast becomes a percent error estimate.
15. The curves for $f = 0$ (for all the Univariance I curves) and $f = 1.0$ c/SD [for Fig. 1(c)] are plotted.
16. The ideal observer prediction is plotted for Fig. 1(c).

APPENDIX B

Test-pedestal Ideal Observer

Consider a Gaussian bar given by

$$G(x) = A\exp(-x^2/2\sigma^2) \quad (1)$$

According to the test-pedestal approach a small change in position would be visible when the difference between the Gaussian, $G(x)$, and the shifted Gaussian, $G(x + \Delta x)$, is just visible. This difference pattern (the test pattern) at location x is given by:

$$\Delta G(x) = G(x + \Delta x) - G(x) \approx A\exp(-x^2/2\sigma^2)\Delta x x/\sigma^2 \quad (2)$$

One version of an ideal observer rule would use a peak–trough threshold. Since the maximum and minimum of Eqn (4) are at $x = \pm\sigma$, this ideal observer's response would be:

$$\Delta G_{\text{ideal position}} = \Delta G(\sigma) - \Delta G(-\sigma) = 2A\exp(-0.5)\Delta x/\sigma \quad (3)$$

Similarly, the contrast discrimination judgment would be based on ΔA, the change in A evaluated at the peak, since that is where the maximum occurs. Thus for contrast discrimination we have:

$$\Delta G_{\text{ideal contrast}} = \Delta A \quad (4)$$

If the ideal observer is equally efficient at both tasks, Eqn (3) and (4) can be equated leading to a proportional connection between position acuity and contrast discrimination:

$$\Delta x/\sigma \approx 0.8\Delta A/A. \quad (5)$$

This prediction is shown as the straight line in Fig. 1(b). We refer to this type of prediction as an ideal observer prediction. Instead of using photon noise to place limits on the ideal observer's threshold, we use the contrast discrimination task to calibrate the observer's sensitivity.

Hu *et al.* (1993). have given similar argument for the connection between contrast and position for sinusoidal gratings rather than Gaussian lines. For a grating whose spatial frequency is f rad/deg the position threshold is given by:

$$\Delta x f \approx \Delta A/A \quad (6)$$

where A is the contrast of the grating. The important feature of the test-pedestal prediction is that the position threshold is linearly proportional to the contrast threshold. The prediction is shown as the upper line in Fig. 1(a).